

Synthesis of visible-light-active nanosize rutile titania photocatalyst by low temperature dissolution–reprecipitation process

Shu Yin^{a,*}, Hitoshi Hasegawa^a, Daisaku Maeda^b, Masayuki Ishitsuka^b, Tsugio Sato^a

^a Institute of Multidisciplinary Research for Advanced Materials, Tohoku University, Sendai 980-8577, Japan

^b New Technology Research Laboratory, Sumitomo Osaka Cement Co. Ltd., 585 Toyotomi-cho, Funabashi-shi, Chiba 274-8601, Japan

Received 24 February 2003; received in revised form 30 April 2003; accepted 4 June 2003

Abstract

Titania nanocrystals were prepared by a “low temperature dissolution–reprecipitation process” (LTDRP) in liquid media. The crystallization of amorphous precursor could proceed at low temperature around room temperature, which was much lower than those of conventional calcination and hydrothermal reactions. The thermodynamically stable rutile formed at low temperature below 70 °C, while the metastable anatase formed at higher temperature. The phase composition, microstructure, morphology, and specific surface area of titania changed significantly depending on the reprecipitation temperatures. Needle-like rutile titania and spherical anatase titania crystals with high specific surface areas were prepared. Well-crystallized needle-like nanosize rutile crystals possessed higher photocatalytic activities than those of anatase crystals under visible light irradiation of wavelength >400 and/or >510 nm.

© 2004 Elsevier B.V. All rights reserved.

Keywords: Visible-light-active photocatalyst; Nanosize rutile titania; Low temperature dissolution–reprecipitation process; Hydrogen evolution; Nitrogen monoxide destruction

1. Introduction

Titania is the most effective photocatalyst and widely applied in purification of air and water, solar system, etc. [1,2]. Three polymorphs, rutile, anatase, and brookite have been occurred in nature. In photocatalysis research, anatase titania is usually considered to be more active than rutile crystalline [3,4]. The enhancement is ascribable to the differences of the Fermi level and the extents of surface hydroxylation of the solid [4]. In addition, rutile usually showed harder agglomeration and larger particle size than those of anatase since rutile is normally prepared by calcination of anatase at high temperatures. Rutile is a thermodynamically stable phase and possesses a smaller band gap than that of anatase phase. Consequently, rutile titania possesses better photo-absorption property in visible light wavelength range (>400 nm). In the present research, titania crystal was prepared from titanium tetraisopropoxide precursor by the low temperature dissolution–reprecipitation process (LTDRP) [5,6] in liquid media under mild conditions. By this novel process, the thermodynamically stable rutile phase with fine particle size and high specific surface area can be prepared even around room

temperature. The phase composition, microstructure, morphology, and specific surface area of titania prepared under various conditions were examined in detail. The hydrogen evolution activity and nitrogen monoxide destruction ability of prepared titania under visible light irradiation were investigated.

2. Experimental

Amorphous TiO₂ gel was prepared by slowly adding 0.125–0.250 mol of titanium tetraisopropoxide to 1000 cm³ of distilled water at room temperature. Transparent acidic TiO₂ colloid solution was obtained by adding hydrochloric acid in the fresh prepared amorphous slurry and stirring at room temperature for 4 h. After aging at desired temperature (25–220 °C) for desired time, fine crystals of titania were produced. The phase constitution of the products was determined by X-ray diffraction (XRD) analysis (Shimadzu, XD-D1). The molar ratios of anatase and rutile were determined by the XRD peak intensity ratio according to Spurr and Myers's method [7]:

$$W_R = \frac{1}{1 + 0.8(I_A/I_R)} \quad (1)$$

$$W_A = 1 - W_R \quad (2)$$

* Corresponding author. Tel.: +81-22-217-5598; fax: +81-22-217-5599.
E-mail address: shuyin@tagen.tohoku.ac.jp (S. Yin).

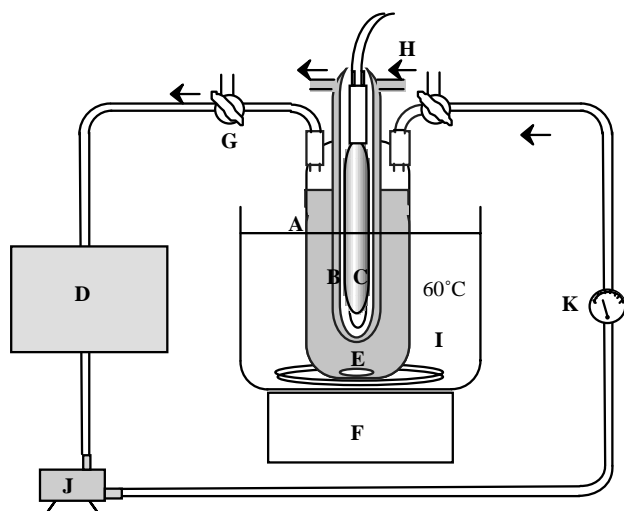


Fig. 1. Schematic illustration of the reaction apparatus used for hydrogen evolution under visible light irradiation: (A) Pyrex reactor (1250 cm^3); (B) Pyrex jacket; (C) 450 W high-pressure mercury lamp; (D) gas chromatography; (E) magnetic stirrer; (F) temperature controller; (G) three-way cock; (H) cooling and filter solution (1 M NaNO_2); (I) heater; (J) gas pump; (K) flow meter. The reactor chamber was replaced by N_2 gas before light irradiation.

where W_A and W_R are the mole fractions of anatase and rutile, I_A and I_R the peak intensities of anatase $d(101)$ and that of rutile $d(110)$. The specific surface areas were determined by the amount of nitrogen adsorption at $-196\text{ }^\circ\text{C}$ (Quantachrome, NOVA 1000-TS). The microstructure of the powder was observed by transmission electron micrograph (TEM, JEOL, JEM-2000EX II) at 200 kV. Band gaps were determined by UV–visible spectrophotometer (Shimadzu, UV-2100). The photocatalytic reaction was carried out in a Pyrex reactor of 1250 cm^3 capacity attached to an inner radiation type 450 W high-pressure mercury lamp. Fig. 1 shows the experimental apparatus used for photocatalytic hydrogen evolution reaction. The inner cell, which served to filter out the UV emission of the mercury arc below 400 nm, had thermostatic NaNO_2 solution flowing through a Pyrex jacket between the mercury lamp and the reaction chamber. The reactor chamber was replaced by nitrogen gas before photocatalytic reaction. Evolved H_2 gas was measured by a gas chromatography (Shimadzu, GC-8A) during the irradiation of the suspension of catalyst in 10 vol.% methanol solution at $60\text{ }^\circ\text{C}$. The methanol acts as a sacrificial substance. The photocatalytic activity for nitrogen monoxide destruction was determined by measuring the concentration of NO

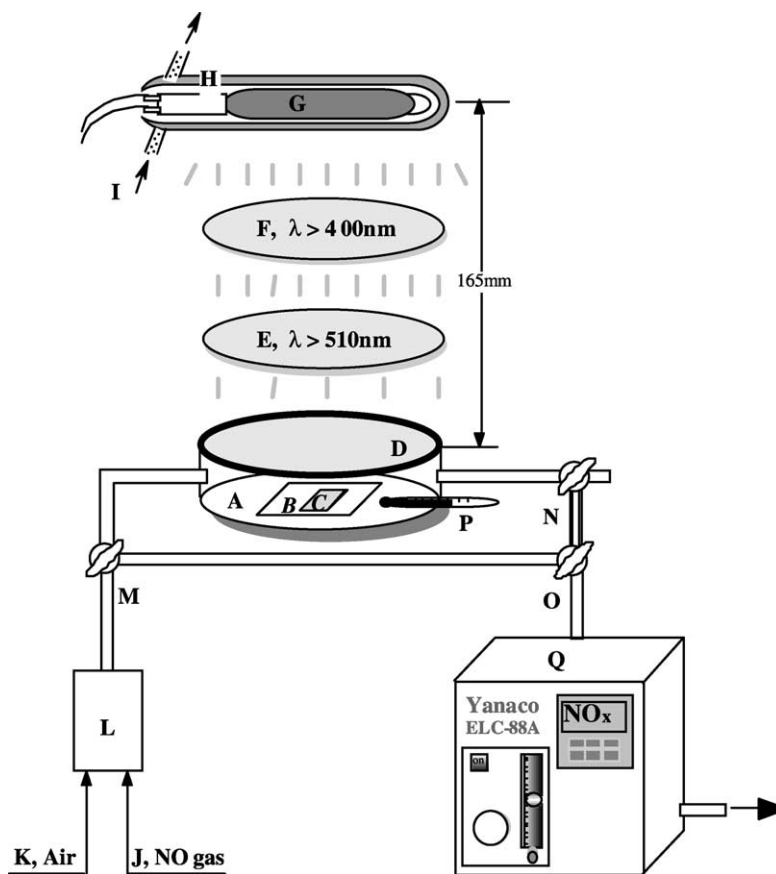


Fig. 2. Experimental apparatus used for photocatalytic destruction of nitrogen monoxide: (A) sealed opaque reactor (plastic, 373 cm^3); (B) glass holder; (C) catalyst ($20\text{ mm} \times 16\text{ mm} \times 0.5\text{ mm}$); (D) colorless and transparent plastic cover; (E) 510 nm cut off filter (Fuji, triacetyl cellulose); (F) 400 nm cut off filter (Kenko, L41 Super Pro(W)); (G) 450 W high-pressure mercury lamp; (H) Pyrex jacket (cut off the light $\lambda < 290\text{ nm}$); (I) cooling water ($30\text{ }^\circ\text{C}$); (J) 2 ppm standard NO gas (flow rate: 100 ml/min); (K) air (flow rate: 100 ml/min); (L) gas mixer; (M)–(O) three-way cock; (P) thermometer; (Q) NO_x analyzer (Yanaco, ECL-88A).

gas at the outlet of a reactor (373 cm^3) during the photo irradiation of constant flowed 1 ppm NO–50 vol.% air mixed (balance N_2) gas ($200 \text{ cm}^3/\text{min}$). Fig. 2 shows the experimental apparatus used for photocatalytic destruction of nitrogen monoxide. As illustrated in this figure, the photocatalyst was placed in a hollow place of $20 \text{ mm} \times 15 \text{ mm} \times 0.5 \text{ mm}$ on a glass holder/plate and set in the center of the reactor. A 450 W high-pressure mercury lamp was used as the light source, where the light wavelength was controlled by selecting various filters. For comparison, the photocatalytic activities of two kinds of commercial titania powder (P25, Degussa; ST-01, Ishihara Industry) were also determined.

3. Results and discussion

It was found that fresh prepared amorphous titania could be dissolved as transparent titania gel in stirred acidic solutions, and then fine particles reprecipitated after a long time (48 h) aging at room temperature. At higher temperatures, the reprecipitation could be realized within 4 h. The precipitation yields of prepared samples were about 20–30%. In order to investigate the effect of co-existed ions, a washing operation was also carried out before and after LTDRP followed by hydrothermal treatment at 220°C .

Table 1 summarized the preparation conditions of the samples. The sample HT220 was prepared by washing amorphous precursor followed by hydrothermal treatment at 220°C . The sample LTDRP25–HT220 was prepared by washing LTDRP25 powders with distilled water followed by hydrothermal treatment at 220°C .

Figs. 3 and 4 show the XRD patterns and TEM photographs of the powders prepared under different conditions listed in Table 1. It is obvious that reprecipitation temperature greatly affected the phase composition and morphology of the final titania powders. The needle-like pure rutile powders with different aspect ratios were obtained at 25 and 50°C . Pure anatase phase with spherical morphology (diameter $\approx 6 \text{ nm}$) was formed at 140°C . The powders prepared by LTDRP at 220°C showed a mixture of rod-like and spherical particles corresponding to rutile and anatase phase. The phase compositional and morphological

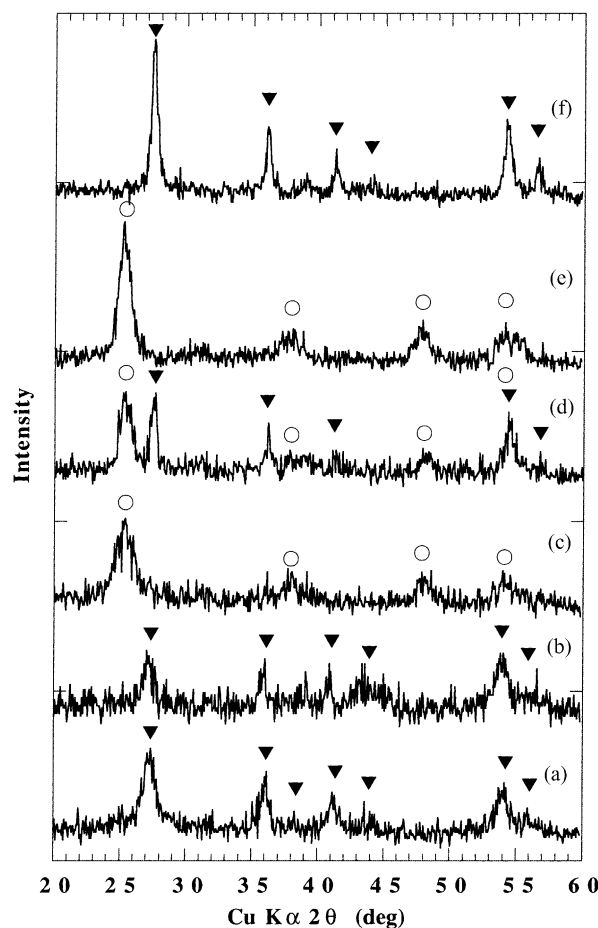


Fig. 3. XRD patterns of the powders prepared by LTDRP in 0.5 M HCl solution at: (a) 25°C for 48 h; (b) 50°C ; (c) 140°C ; (d) 220°C for 4 h; and those prepared by hydrothermal treatment in water at 220°C for 4 h using (e) the amorphous precursor washed with distilled water; (f) the sample (a) washed with distilled water; (\blacktriangledown) rutile; (\circ) anatase.

control of titania nanoparticles might also be realized by combining LTDRP with the washing operation followed by hydrothermal treatment in liquid media. The hydrothermal treatment of amorphous precursor that washed with distilled water only produced anatase phase with spherical morphology. However, if the rutile precursor prepared from LTDRP at 25°C was washed, rod-like rutile phase with high

Table 1
Preparation conditions of titania powders

Sample	Solvent	Autoclaving conditions		Washing operation ^a	Comment
		Temperature ($^\circ\text{C}$)	Time (h)		
LTDRP25	0.5 M HCl solution	25	48	No	Part (a) of Figs. 3 and 4
LTDRP50	0.5 M HCl solution	50	4	No	Part (b) of Figs. 3 and 4
LTDRP140	0.5 M HCl solution	140	4	No	Part (c) of Figs. 3 and 4
LTDRP220	0.5 M HCl solution	220	4	No	Part (d) of Figs. 3 and 4
HT220	Distilled water	220	4	Yes/before	Part (e) of Figs. 3 and 4
LTDRP25–HT220	0.5 M HCl–water	220	4	Yes/after	Part (f) of Figs. 3 and 4
P25	–	–	–	–	Commercial powder
ST-01	–	–	–	–	Commercial powder

^a Before or after LTDRP at 25°C .

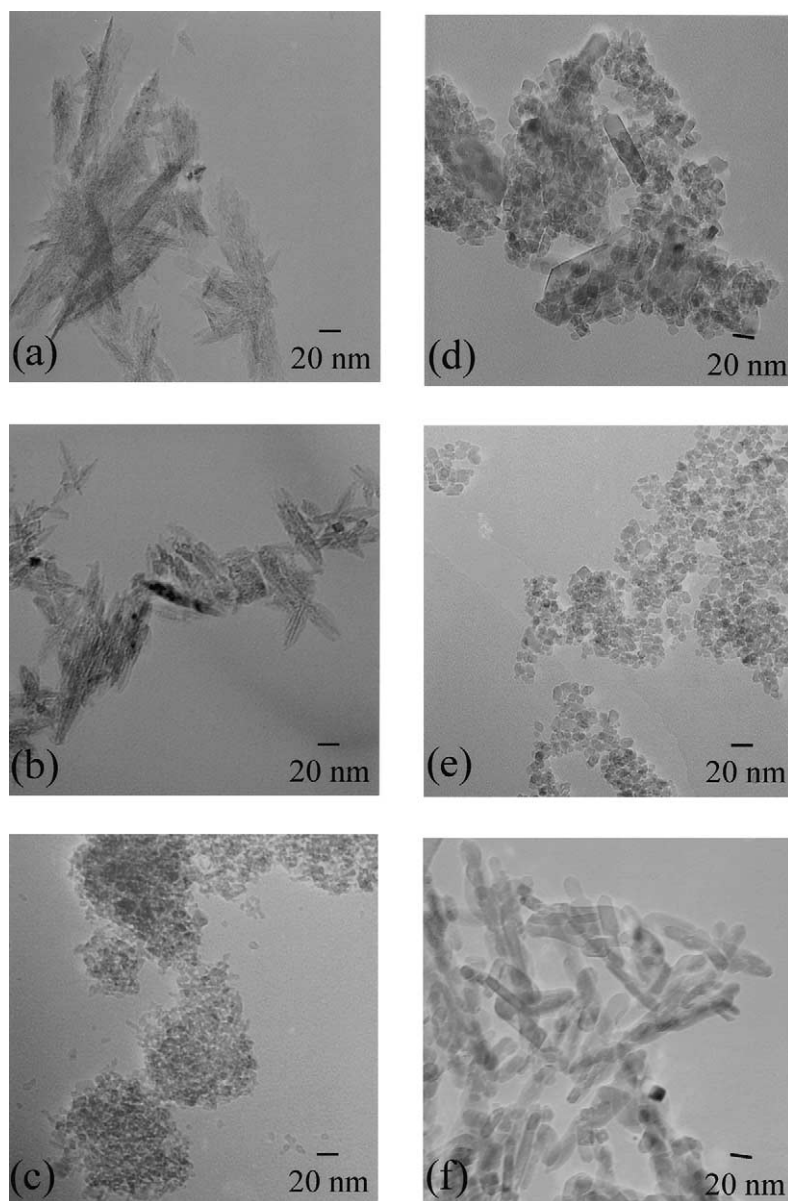


Fig. 4. TEM photographs of the powders prepared by LTDRP in 0.5 M HCl solution at: (a) 25 °C for 48 h; (b) 50 °C for 4 h; (c) 140 °C for 4 h; (d) 220 °C for 4 h, and those by hydrothermal treatment at 220 °C for 4 h (e) using the amorphous precursor washed with distilled water; (f) using the precursor from LTDRP in HCl at 25 °C followed by washing with distilled water.

crystallinity was formed after the hydrothermal treatment at the same temperature (parts (e) and (f) of Figs. 3 and 4).

Fig. 5 shows the mole fraction of rutile phase formed by LTDRP at various precipitation temperatures with different Ti/HCl ratio. Pure rutile formed between room temperature and 70 °C, and the products consisting of the mixture of rutile and anatase formed above 70 °C. The mole fraction of rutile decreased with increasing treatment temperature. Pure anatase could be obtained at 150–170 °C. However, the rutile phase fraction increased at temperatures above 170 °C. In order to explain the complex crystallization behavior of titania prepared by the LTDRP, a formation mechanism was proposed and shown in Fig. 6.

When titanium tetraisopropoxide was added in distilled water, hydrolysis reaction proceeded fast leading to the formation of amorphous $\text{Ti}(\text{OH})_4$ precipitate. As mentioned above, the amorphous titania could be dissolved as transparent titania gel in stirred acidic solutions, and then fine particles reprecipitated after aging at desired temperatures. It is known that titanium did not exist in the form of Ti^{4+} cation, but existed as a sixfold coordinated $[\text{Ti}(\text{H}_2\text{O})_6]^{4+}$ complex [8,9]. It is accepted that both anatase and rutile titania can grow from TiO_6 octahedra, and the phase formation proceeds by the rearrangement of the octahedra. In the present research, the rutile phase content decreased with increasing the treatment temperature of LTDRP at first, and

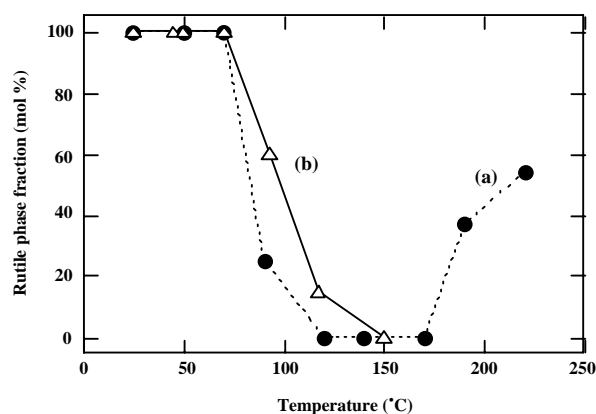


Fig. 5. The mole fraction of rutile phase in titania powders prepared by LTDRP in 0.5 M HCl solution with: (a) Ti:HCl ratio = 1:4; (b) Ti:HCl ratio = 1:2 at various precipitation temperatures.

then increased at higher temperatures. The reason might be explained by the different ion product values in the solution at various temperatures. It is well known that the ionic product of water ($K_{w,25^\circ\text{C}}$) is equal to 1.0×10^{-14} , i.e. $[\text{OH}^-] = 2.0 \times 10^{-14}$ in the case of $[\text{H}^+] = 0.5 \text{ mol/l}$ at 25°C . While, the ionic product of water changes significantly with temperature. For example, the value of ionic product of water at 140°C ($K_{w,140^\circ\text{C}}$) greatly increases to about 1.6×10^{-12} . In this case, $[\text{OH}^-] = 3.2 \times 10^{-12}$, which is about 160 times higher than that at 25°C [10]. During the reprecipitation and the rearrangement of the titanium oxide structure, $[\text{Ti}(\text{H}_2\text{O})_6]^{4+}$ hydrated ions were dehydrated and polymerized to $[(\text{H}_2\text{O})_5\text{Ti}(\text{OH})]_n^{3+}$ or $[(\text{H}_2\text{O})_4\text{Ti}(\text{OH})_2]_n^{2+}$ [8,9] under different amounts of OH^- ion, and finally formed TiO_6 octahedra. In the case of less OH^- amount (ex. 25°C), the TiO_6 octahedra preferred to form corner-sharing structure, while in the case of more OH^- amount (ex. 140°C), the TiO_6 octahedra preferred to form edge-sharing structure. As a result, rutile phase sharing more corners and less edges with neighboring octahedra formed at low temperatures below 70°C . On the other hand, anatase structure sharing less corners and more edges with neighboring octahedra formed at higher temperatures.

Above 170°C , part of the thermodynamically metastable anatase phase transformed to stable rutile phase and led to the increase of rutile phase content. Similarly, it was reported that higher acidity was beneficial for the formation of rutile phase, while lower acidity was favorable for the formation of anatase phase under hydrothermal conditions [11].

In the absence of hydrochloric acid, $[\text{H}^+] = [\text{OH}^-] \geq 1.0 \times 10^{-7}$. Only pure anatase phase was produced even under high temperature of 220°C (HT220), while the crystallization under such low temperature as 25°C could not be carried out because the amorphous precipitate could not be dissolved as hydrated ion under this condition. Once rutile had formed, only rutile phase would be produced even under the same condition of $[\text{H}^+] = [\text{OH}^-] \geq 1.0 \times 10^{-7}$ because rutile nanocrystals acted as crystal seeds during the crystallization process (LTDRP25-HT220).

The phase composition, morphology, specific surface area, together with the band gap value and photocatalytic hydrogen evolution activity of the prepared titania powders are summarized in Table 2. It was indicated that rutile prepared by LTDRP possessed needle-like and rod-like morphology, while anatase possessed spherical morphology in the present research. The powders prepared in HCl solution at low temperatures possessed rutile phase with specific surface area larger than $100 \text{ m}^2/\text{g}$. Meanwhile, the anatase particles formed in HCl solution possessed relatively higher specific surface area such as $212.0 \text{ m}^2/\text{g}$. The powders with anatase phase showed band gap values of 3.06–3.11 eV, which corresponds to the wavelength of 398–405 nm. The rutile powders showed relatively smaller band gap values of 2.99–3.02 eV, which corresponds to the wavelength of 410–415 nm. It was found that rutile phase prepared by the present process possessed such high hydrogen evolution activity as $56.0 \mu\text{mol/h}$, whereas anatase phase showed almost no hydrogen evolution activity under visible light irradiation ($\lambda > 400 \text{ nm}$). It is suggested that visible light induced activity of rutile is caused by its small band gap value ($< 3.02 \text{ eV}$, corresponding to light wavelength $> 410 \text{ nm}$). In addition, the large specific surface area and small particle size of the rutile prepared in the present research might also act as some important roles during the photocatalytic

Table 2

Effects of operation conditions on phase composition, morphology, specific surface area, band gap and photocatalytic activities of the prepared titania powders

Sample	Phase composition ^a	Morphology	BET SSA (m^2/g)	Band gap (eV)	Hydrogen evolution activity ($\mu\text{mol/h}$) ^b
LTDRP25	R	Needle-like	135.0	3.01	9.5
LTDRP50	R	Needle-like	106.0	3.01	56.0
LTDRP140	A	Spherical	212.0	3.06	0.0
LTDRP220	A + R	Rod-like + spherical	94.3	3.02	52.0
HT220	A	Spherical	142.0	3.11	0.0
LTDRP25-HT220	R	Rod-like	65.2	3.00	23.0
P25	A + R	Spherical	47.0	2.98	33.0
ST-01	A	Spherical	309.0	3.10	2.0

^a R: rutile phase; A: anatase phase.

^b Under visible light irradiation ($\lambda > 400 \text{ nm}$).

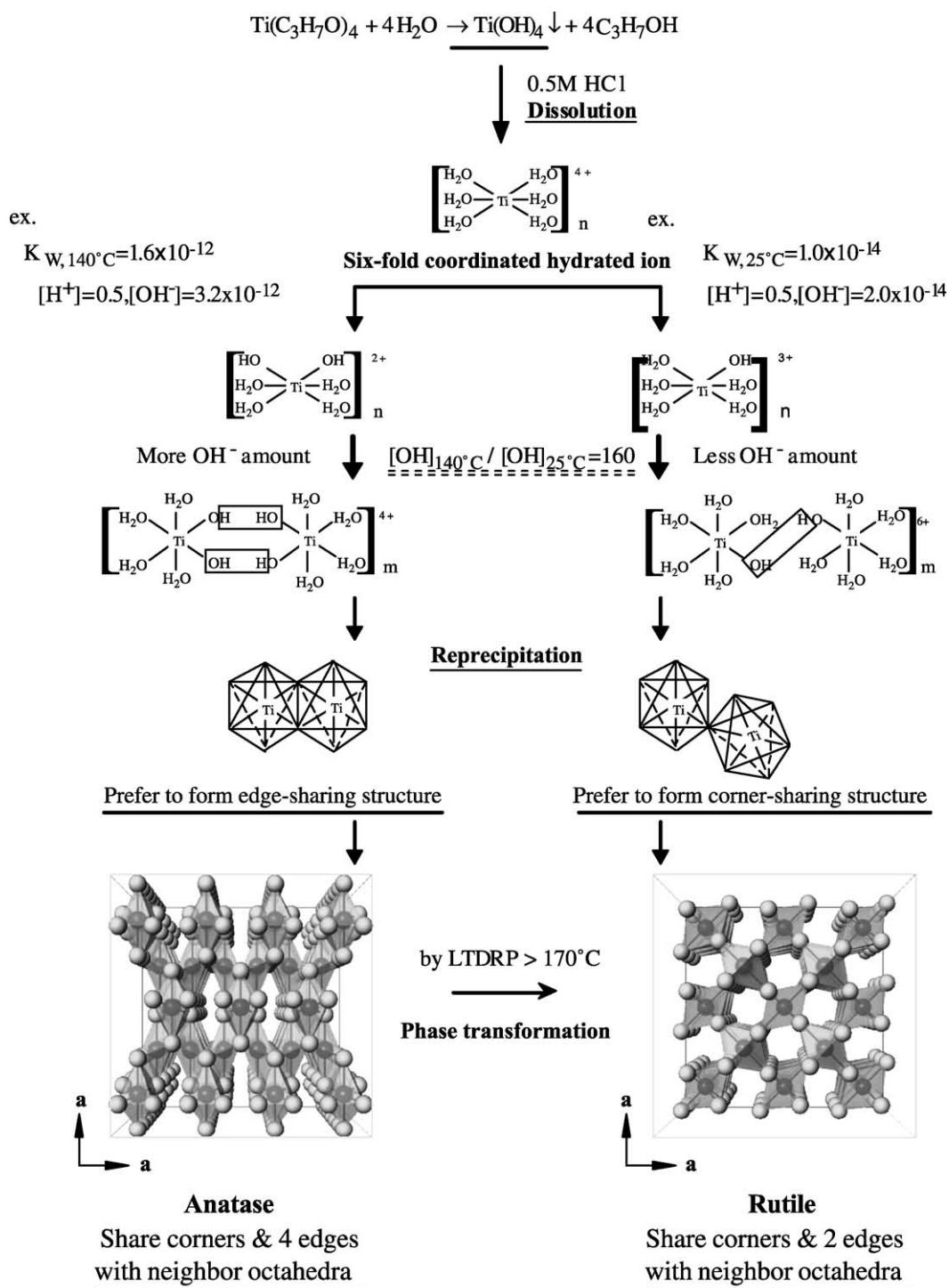


Fig. 6. Formation mechanism of titania nanocrystals prepared by LTDRP.

reaction, remember normal rutile powder usually possesses comparatively large particle size.

Fig. 7 shows the nitrogen monoxide destruction ability of the powders prepared by LTDRP at different temperatures together with that of commercial powder P25 titania under different wavelength of light irradiation. The result of blank test without titania powder was indicated by dotted lines.

It is accepted that electron/hole pairs are formed by the photo-excitation of titania. In the presence of oxygen, the electrons in the conduction band are immediately trapped by the molecular oxygen to form $\bullet\text{O}_2^-$, which can then generate active $\bullet\text{OOH}$ radicals. The nitrogen monoxide reacts with these reactive oxygen radicals, molecular oxygen, and very small amount of water in air to produce HNO_2 or

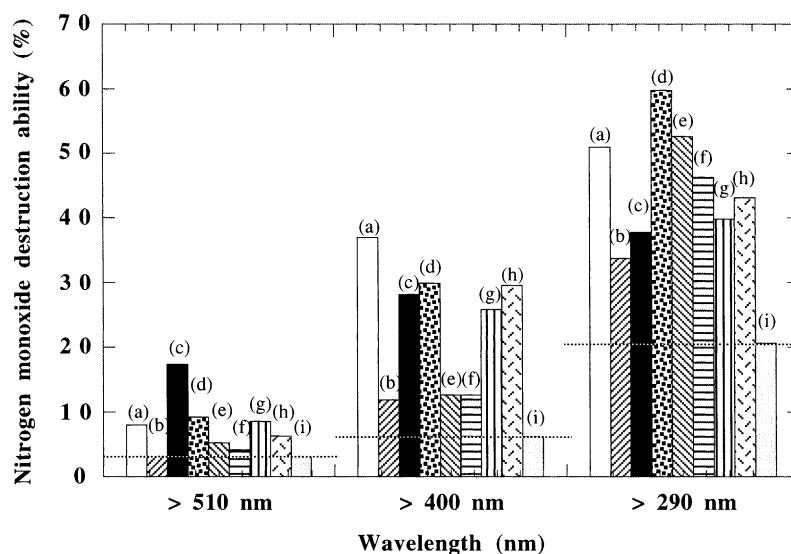


Fig. 7. Nitrogen monoxide destruction ability of (a) P25 titania and the powders prepared by LTDRP at: (b) 25 °C; (c) 50 °C; (d) 90 °C; (e) 120 °C; (f) 140 °C; (g) 170 °C; (h) 190 °C under different wavelengths of light irradiation; (i) blank (without catalyst).

HNO_3 . About 17, 28 and 38% of nitrogen monoxide were continuously destructed by using the rutile titania prepared from LTDRP at 60 °C under the irradiation of visible light of $\lambda > 510$, >400 nm, and near-UV light of $\lambda > 290$ nm, respectively. On the other hand, the mixture of anatase and rutile prepared by LTDRP at 90 °C possessed excellent nitrogen monoxide destruction ability under near-UV light irradiation. Similar to the results of hydrogen evolution activity, low nitrogen monoxide destruction ability were observed by using pure anatase phase titania (Fig. 7(e)–(g)), indicating that rutile phase with nanosize and high specific surface area possessed higher photocatalytic activities than those of anatase phase. The lowest photocatalytic activities of the rutile powder LTDRP25 was suspected by the existence of hydrous structure, because it was prepared at such low temperature as 25 °C. Although the activity under irradiation of light wavelength >510 nm was observed in the present research, the reason was not clarified yet. The wavelength was far away from band gap excitation. Similarly, it was reported that onset of the action spectra of TiO_2 photocatalytic reaction shifted very much to longer wavelength side compared with that of diffuse reflectance spectra [12,13]. The shift value depended on the kind of photocatalytic reaction. Unfortunately, the detail mechanism was not so clear either. With the existing state of affairs, further investigation is required.

Fig. 8 shows the relationship among phase composition, photocatalytic nitrogen monoxide destruction ability and LTDRP temperature under different wavelength of light irradiation. The data of LTDRP25 was not plotted in this figure. The photocatalytic activity under visible light irradiation showed almost the same behaviors with those of rutile content. On the other hand, the photocatalytic activity under near-UV light irradiation showed different profiles, which might be

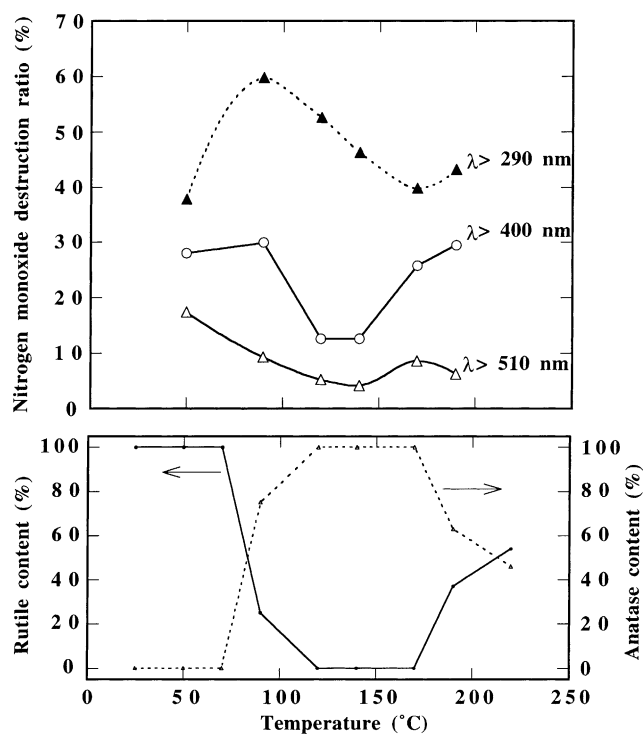


Fig. 8. The relationship among LTDRP temperature, phase composition and photocatalytic nitrogen monoxide destruction ability under different wavelengths of light irradiation.

caused by the high photocatalytic activity of anatase in UV light region. It is obvious that well-crystallized rutile powder with high specific surface area possessed higher photocatalytic activities, including hydrogen evolution activity and nitrogen monoxide destruction ability, than those of anatase phase.

4. Conclusions

Based on the experimental results the following conclusions may be drawn:

- (1) Crystallization of rutile and anatase titania was realized at very low temperature by the LTDRP.
- (2) The phase compositional and morphological control of titania powders could be realized by applying washing operation and/or hydrothermal treatment to LTDRP process.
- (3) A formation mechanism of titania nanocrystals prepared by LTDRP was suggested.
- (4) Well-crystallized nanosize rutile titania possessed higher hydrogen evolution activity and nitrogen monoxide destruction ability than those of anatase under visible light irradiation.

Acknowledgements

This work was partly supported by a grant in aid for Scientific Research, No. 14750660, from the Ministry of Education, Science and Culture.

References

- [1] A. Fujishima, K. Honda, *Nature* 238 (1972) 37–38.
- [2] B. O'Regan, M. Gratzel, *Nature* 353 (1991) 737–739.
- [3] J. Augustynski, *Electrochim. Acta* 38 (1993) 43–46.
- [4] R.I. Bickley, T. Gonzalez-Carreno, J.S. Lees, L. Palmisano, R.J. Tilley, *J. Solid State Chem.* 92 (1991) 178–190.
- [5] S. Yin, R. Li, Q. He, T. Sato, *Mater. Chem. Phys.* 75 (2002) 76–80.
- [6] S. Yin, H. Hasegawa, T. Sato, *Chem. Lett.* (2002) 564–565.
- [7] R.A. Spurr, W. Myers, *Anal. Chem.* 29 (1957) 760–762.
- [8] T. Maki, *Nippon Kagaku Kaishi* 8 (1978) 945–955.
- [9] Y. Zhang, E. Shi, Z. Chen, W. Li, X. Hu, *J. Mater. Chem.* 11 (2001) 1547–1551.
- [10] D.R. Lide (Ed.), *Handbook of Chemistry and Physics*, 76th ed., CRC Press, New York, 1995–1996, pp. 8–56.
- [11] H. Cheng, J. Ma, Z. Zhao, L. Qi, *Chem. Mater.* 7 (1995) 663–671.
- [12] T. Torimoto, N. Nakamura, S. Ikeda, B. Ohtani, *Phys. Chem. Chem. Phys.* 4 (2002) 5910–5914.
- [13] B. Ohtani, Y. Aburakawa, S. Ikeda, T. Torimoto, *Proceedings of the 83rd CSJ National Meeting, Abstract Book, vol. I, Chemical Society of Japan, Tokyo, 2003, p. 171. ISSN 0285-7626.*